Environ. Sci. Technol. **2004**, *38,* 1888−1896

Removal of Natural Hormones by Nanofiltration Membranes: Measurement, Modeling, and Mechanisms

LONG D. NGHIEM,[†,‡] ANDREA I. SCHÄFER,[‡] AND MENACHEM ELIMELECH*[,†]

Department of Chemical Engineering, Environmental Engineering Program, Yale University, New Haven, Connecticut 06520-8286, and Environmental Engineering, University of Wollongong, New South Wales 2522, Australia

The removal mechanisms of four natural steroid hormones—estradiol, estrone, testosterone, and progesterone—by nanofiltration (NF) membranes were investigated. Two nanofiltration membranes with quite different permeabilities and salt retention characteristics were utilized. To better understand hormone removal mechanisms, the membrane average pore size was determined from retention data of inert organic solutes of various molecular weights and a pore transport model that incorporates steric (size) exclusion and hindered convection and diffusion. Results indicate that, at the early stages of filtration, adsorption (or partitioning) of hormones to the membrane polymer is the dominant removal mechanism. Because the adsorptive capacity of the membrane is limited, the final retention stabilizes when the adsorption of hormones into the membrane polymer has reached equilibrium. At this later filtration stage, the overall hormone retention is lower than that expected based solely on the size exclusion mechanism. This behavior is attributed to partitioning and subsequent diffusion of hormone molecules in the membrane polymeric phase, which ultimately results in a lower retention. Hormone diffusion in the membrane polymeric matrix most likely depends on the size of the hormone molecule, hydrogen bonding of hormones to membrane functional groups, and hydrophobic interactions of the hormone with the membrane polymeric matrix.

Introduction

Natural steroid hormones are continuously released to the environment by humans and animals, both directly and indirectly during the discharge of treated domestic wastewater effluents. Removal efficiency of hormones by conventional wastewater treatment plants varies largely, but the overall removal is generally quite low (*1*). Consequently, such contaminants are present in all freshwater bodies receiving treated wastewater effluents (*2*−*5*). A recent study by the U.S. Geological Survey (*2*) provides compelling evidence of the widespread presence of both natural and synthetic steroid hormones in U.S. surface waters susceptible to contamination by wastewater effluents.

Steroid hormones have the greatest endocrine-disrupting potency among all endocrine disrupting chemicals (EDCs) (*6*). For instance, it has been reported that estradiol concentrations as low as 1 ng/L show a clear endocrine-disrupting effect on fish (*6*). Laboratory and field studies have provided ample evidence of the effects of endocrine disruption on various species, including fish, amphibians, birds, reptiles, and mammals (*6*−*10*). Several studies also suggest a link between human exposure to EDCs and decrease in male sperm counts; increases in testicular, prostate, ovarian, and breast cancer; and reproductive malfunctions (*11*−*13*). More importantly, public concern and uncertainty regarding potential long-term health effects present major obstacles to the widespread implementation of domestic wastewater reuse as a means to alleviate growing pressure on available freshwater resources (*14*).

Removal of trace organics by pressure-driven membrane processes has been the subject of several recent studies. It has been demonstrated that nanofiltration membranes can be used to remove pesticides and that the removal mechanisms are mainly influenced by steric and electrostatic interactions (*15, 16*). However, other solute and membrane physicochemical properties may also influence the separation behavior. Van der Bruggen et al. (*17*) reported that a high dipole moment of the organic solute could induce a lower retention than what expected based only on size exclusion mechanism. In another study, Kiso et al. (*18*) suggested that adsorption of hydrophobic pesticides to the membrane can enhance retention, although such enhancement was probably limited to a relatively short time scale.

Studies on the removal of natural hormones by pressure-driven membrane processes are rather scarce. Consequently, the fundamental mechanisms governing hormone retention by nanofiltration membranes are not well understood. It has been recently reported that steroid hormones can adsorb (partition) onto the membrane to some extent, presumably aided by hydrogen bonding or hydrophobic interaction with the membrane polymer (*19, 20*). Schäfer et al. (*19*) argued that both size exclusion and adsorption are essential in maintaining high initial retention by nanofiltration membranes that otherwise exhibit relatively high salt passage. However, little is known about the effect of adsorption on the overall long-term hormone retention, especially when adsorption has reached equilibrium. Thus, a fundamental understanding of the removal mechanisms of hormones by pressure-driven membrane processes is of paramount importance.

This study aimed at elucidating the removal mechanisms of natural steroid hormones by NF membranes. Filtration experiments were carried out with four natural hormones and two NF membranes having different water and salt permeabilities. Hormone retention was related to the membrane and hormone molecule physicochemical properties, and the mechanisms of hormone retention and transport through the NF membrane were delineated and discussed.

Theory

Unlike reverse osmosis membranes, it is widely accepted that nanofiltration membranes are porous. Consequently, a hydrodynamic approach for modeling solute transport in a nanoporous membrane will be utilized in this paper. The hydrodynamic approach differs fundamentally from the

* Corresponding author telephone: (203)432-2789; fax: (203)432-2881; e-mail: menachem.elemelech@yale.edu.
† Yale University.
‡ University of Wollongong.

10.1021/es034952r CCC: $27.50

Published on Web 02/13/2004

classical thermodynamic approach commonly used in reverse osmosis. While the thermodynamic approach considers the membrane to be a "black box" when deriving the phenomenological equations (*21*), the hydrodynamic approach assumes a geometrical model of a membrane and derives all the transport equations and properties based on this geometry (*22*).

In the present model, the NF membrane is modeled as a bundle of cylindrical capillary tubes, all having the same radius. Furthermore, we assume a spherical solute particle, as is the case with all microscopic transport models involving low molecular weight solutes (*22*). Although it is possible to determine the dimensions (length and width) of a rigid organic solute (*23*, *24*), taking into account such dimensions would result in a much more intricate model. Our spherical solute assumption also accounts for the fact that the solute enters the membrane pore in a random rather than an orientated fashion. The key equations of the hydrodynamic theory leading to an analytical expression for solute rejection by a nanoporous membrane are delineated below.

Solute Transport through a Nanoporous Membrane. The solute flux in a cylindrical pore can be expressed as the sum of diffusive and convective contributions (*22*, *25*):

$$J_s = -K^{-1}D_\infty\frac{\partial c}{\partial z} + GVc \tag{1}$$

Here, J_s is the solute flux, V is the unperturbed fluid velocity, c is the solute concentration, D_∞ is the Stokes−Einstein diffusion coefficient, z is the axial position along the cylindrical pore, K is the enhanced drag, and G is the lag factor. The hydrodynamic coefficients K and G account for the finite pore size—the pore walls increase the drag on a solute molecule translating parallel to the pore axis ($K > 1$) and cause the velocity of the freely suspended solute to lag behind the approach velocity of the fluid ($G < 1$). Note that K and G depend on the ratio of the solute radius to pore radius, $\lambda = r_s/r_p$ as well as on the radial position in the pore, r, commonly expressed in terms of a dimensionless radial position, $\rho = r/r_p$.

The solute concentration c as well as the variables K, G, and V vary with the radial position ρ. Thus, one has to obtain the radial average solute flux, $\langle J_s\rangle$, by integrating over the pore cross-section. The final result for the radial average solute flux at any axial position z is (*22*)

$$\langle J_s\rangle = -K_d D_\infty\frac{\mathrm{d}\langle c\rangle_z}{\mathrm{d}z} + K_c\langle V\rangle\langle c\rangle_z \tag{2}$$

The term K_dD_∞ is known as the hindered diffusivity in the pore, while the term K_c accounts for the convective effects and may be considered as an effective drag factor.

We can now integrate the radial average solute flux over the entire pore length (or membrane thickness) L. To do this, the solute concentrations within the pore must be related to those outside the pore (in the bulk solution). This can be done using the distribution coefficient, Φ, for hard-sphere particles when only steric interactions are considered (*22*, *26*):

$$\Phi = \frac{\langle c\rangle_0}{c_0} = \frac{\langle c\rangle_L}{c_L} = (1-\lambda)^2 \tag{3}$$

where c_0 and c_L are the solute concentrations just outside the pore entrance and pore exit, respectively, and $\langle c\rangle_0$ and $\langle c\rangle_L$ are the corresponding average concentrations just inside the pore at $z = 0$ and $z = L$, respectively. Thus, integration of eq 2 over the entire pore length (from $z = 0$ to $z = L$), with the boundary conditions from eq 3, yields the macroscopic solute flux equation:

$$\langle J_s\rangle = \frac{\Phi K_c\langle V\rangle c_0[1-(c_L/c_0)\exp(-Pe)]}{1-\exp(-Pe)} \tag{4}$$

where Pe is the membrane Peclet number, defined as

$$Pe = \frac{K_c\langle V\rangle L}{K_d D_\infty} = \frac{K_c\langle J_v\rangle L}{K_d\epsilon D_\infty} \tag{5}$$

In these equations, $\langle V\rangle$ is the radial average fluid velocity in a cylindrical membrane pore, which is equal to the membrane volumetric permeate flux, $\langle J_v\rangle$, divided by the membrane porosity, ϵ.

Solute Retention by Nanoporous Membranes. Relating the solute flux to the fluid velocity and the solute concentration in the permeate:

$$\langle J_s\rangle = \langle V\rangle c_L \tag{6}$$

we can rearrange eq 4 to obtain the so-called sieving coefficient, S_a:

$$S_a = \frac{c_L}{c_0} = \frac{\Phi K_c}{1-\exp(-Pe)(1-\Phi K_c)} \tag{7}$$

where c_0 and c_L are the solute concentrations just outside the pore entrance (i.e., on the membrane surface at the feed side) and pore exit (i.e., permeate side), respectively. The real (or intrinsic) retention is related to the sieving coefficient as

$$R_r = 1 - \frac{c_L}{c_0} = 1 - S_a = 1 - \frac{\Phi K_c}{1-\exp(-Pe)(1-\Phi K_c)} \tag{8}$$

Note that the real retention, R_r, relates the solute permeate concentration to the membrane surface concentration, not the bulk feed concentration. The latter concentrations are different for solute rejecting membranes because of concentration polarization (*27*). Using the film theory for concentration polarization, it can be readily shown that the observed retention, R_o, is related to the real retention via

$$\ln\frac{1-R_r}{R_r} = \ln\frac{1-R_o}{R_o} - \frac{\langle J_v\rangle}{k_f} \tag{9}$$

where k_f is the mass transfer coefficient. The determination of the mass transfer coefficient is described later in Materials and Methods. Note that in this equation, the observed retention, R_o, and the volumetric permeate flux, $\langle J_v\rangle$, are routinely measured during a typical nanofiltration experiment.

Determination of the Hydrodynamic Hindrance Coefficients. To use the above model to calculate solute retention by a nanoporous membrane, the hydrodynamic coefficients K_c and K_d must be determined. While various simplified theoretical expressions are available in the literature, most cover only a small range of λ, which limits their use to ultrafiltration and microfiltration membranes. The most complete expressions, which cover the entire range of λ, were given by Bungay and Brenner (*28*):

$$K_c = \frac{(2-\Phi)K_s}{2K_t} \tag{10a}$$

$$K_d = \frac{6\pi}{K_t} \tag{10b}$$

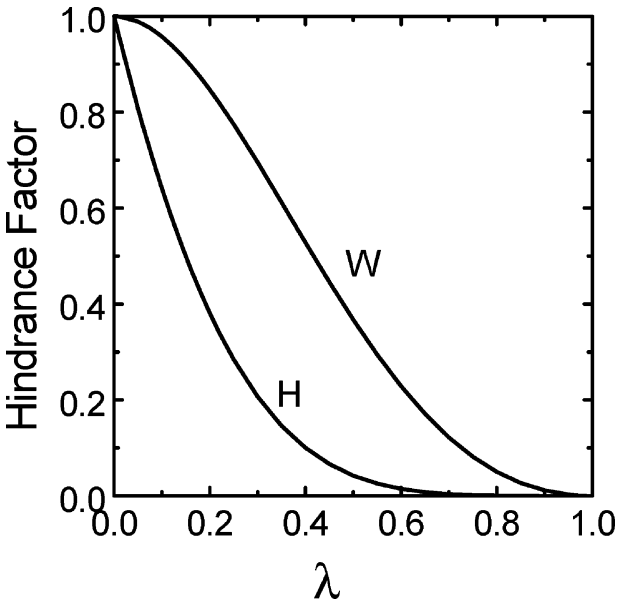

FIGURE 1. Dependence of hindrance factors for diffusion (*H*) and convection (*W*) of a neutral, spherical solute on the ratio of solute size to pore size, λ. The factors *H* and *W* were determined from eqs 3 and 10.

where

$$K_t = \frac{9}{4}\pi^2\sqrt{2}(1-\lambda)^{-5/2}\left[1 + \sum_{n=1}^{2} a_n(1-\lambda)^n\right] + \sum_{n=0}^{4} a_{n+3}\lambda^n \quad (11a)$$

$$K_s = \frac{9}{4}\pi^2\sqrt{2}(1-\lambda)^{-5/2}\left[1 + \sum_{n=1}^{2} b_n(1-\lambda)^n\right] + \sum_{n=0}^{4} b_{n+3}\lambda^n \quad (11b)$$

The coefficients a_n and b_n in this equation, for up to $n = 7$, can be found in ref *28*.

Note that $H = \Phi K_d$ and $W = \Phi K_c$ are termed the hindrance factors for diffusion and convection, respectively. The dependence of these factors on the solute to pore radii ratio, λ ($= r_s/r_p$), calculated from eqs 3 and 10, is described in Figure 1. It is clearly shown that the finite pore size of porous membranes has a dramatic effect on solute diffusion and convection when λ is close to 1. This is quite relevant to nanofiltration membranes where the pore size is not much larger than the solute size.

Materials and Methods

Representative NF Membranes. Two NF membranes, denoted NF-270 and NF-90 (FilmTec Corp., Minneapolis, MN), were used in this investigation. The membranes were received as flat sheets and were stored in deionized water (NanoPure II, Dubuque, IA) at 4 °C. As indicated by the manufacturer, the membranes consist of a semi-aromatic piperazine-based, polyamide layer on top of a microporous polysulfone support (*29*). Both the NF-270 and NF-90 membranes are negatively charged at pH above 3. Sodium chloride retentions by the NF-90 and NF-270 (at 3,000 mg/L NaCl and 4.5 bar) are 85% and 40%, respectively.

Natural Hormones. Four radiolabeled steroid hormones—namely, estradiol, estrone, progesterone, and testosterone—were selected for this study (Figure 2). Estradiol-2,4-^3H-(N) and progesterone-2,4,6,7-3*H*-(N) were purchased from Sigma-Aldrich (Saint Louis, MO), while estrone-2,4,6,7-3*H*-(N) and testosterone-1,2-3*H*-(N) were purchased from Perkin-Elmer (Boston, MA). As seen in Figure 2, all hormones have two

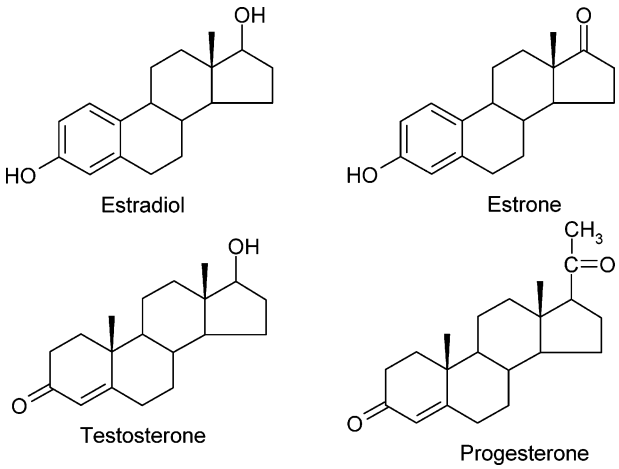

FIGURE 2. Molecular structure of the four natural hormones used in this study.

TABLE 1. Molecular Weight, Diffusivity, and Stokes Radius of Organic Tracers

organic tracer	MW (g/mol)	diffusivity[a] (10^{-10} m^2/s)	Stokes radius[b] (nm)
dioxane	88	9.1	0.234
erythritol	120	8.1	0.263
xylose	150	7.4	0.290
dextrose	180	6.6	0.324

[a] Calculated using the Wilke and Chang equation (*44*) at 20 °C. [b] Calculated using Stokes−Einstein equation.

oxygen-containing functional groups, which take the form of a primary or secondary alcohol or a ketone.

The radiolabeled hormones were supplied in ethanol solution and were diluted with DI water prior to use. Specific radioactivity of estradiol, estrone, progesterone, and testosterone were 17, 65, 88, and 55 Ci/mmol, respectively. The stock solutions were stored in the dark at <4 °C. All hormones have radiochemical purity higher than 97% at the time of purchase. Experiments were completed within 5 months from the time of purchase. According to the manufacturers, it is estimated that the purity decreases approximately 2−5% each year as these are unstable products (*30*, *31*).

Radiolabeled hormones were analyzed using a Perkin-Elmer scintillation counter (Tri-Carb 2900 TR). Scintillation vials (20 mL) were filled with 1 mL of sample and 9 mL of Ultima Gold scintillation cocktail (Perkin-Elmer, Boston, MA). Prior to analysis, the vials were shaken vigorously, and the samples were counted for 5 min. A set of calibration standards at concentrations of 0, 0.01, 0.1, 1, 10, 100, and 1000 ng/L of each hormone were prepared from fresh compounds. Hormone concentration was determined based on a linear regression of the calibration standards. With this method, the detection limit was approximately 0.5 ng/L for estradiol and 0.1−0.2 ng/L for the remainder of the hormones.

Organic Tracers. Low molecular weight, neutraly charged organic molecules—dioxane, erythritol, xylose, and dextrose—were chosen as organic tracers to characterize the average pore size of the NF membranes. These organic solutes are inert and do not adsorb to the membrane. Molecular weights, diffusivities, and Stokes radii of the selected organic tracers are listed in Table 1. A Shimadzu TOC analyzer (TOC V-CSH) was used to analyze the organic tracers. All organic tracers used were of analytical grade and were purchased from Fisher Scientific (Fair Lawn, NJ).

NF Membrane Test Unit. A laboratory-scale, cross-flow membrane filtration test unit was used this study. The unit utilizes a Dayton capacitor start motor (Dayton Electronic

Manufacturing Co., Chicago, IL) coupled with a Hydra-Cell pump (Wanner Engineering Inc., Minneapolis, MN) capable of providing pressures up to 68 bar (1000 psi) and a flow rate of 4.2 L/min. Temperature of the feed reservoir was controlled using a chiller/heater (Neslab RTE 111). Duplicate plate-and-frame membrane cells were used, each housing a membrane coupon with an identical effective surface area of 7.7 × 3.0 cm. Permeate flow rate was monitored by a digital flow meter connected to a PC, and cross-flow rate was monitored by a rotameter. All test unit parts in contact with the solution are made of stainless steel or Teflon to minimize adsorption of the organic compounds used.

Membrane Filtration Protocol. Prior to each experiment, the membrane was stabilized at 12 bar (176.4 psi) using DI water for at least 16 h until the permeate flux attained a constant value. The feed reservoir temperature was kept at 20 ± 0.1 °C throughout the experiment. Unless otherwise stated, permeate was recycled back to the feed reservoir.

To characterize the membrane pore size, a feed solution containing 20 mg/L (as TOC) of each organic tracer in DI water was used. The experiments were conducted at pressures of 4, 6, 8, 10, and 12 bar (58.8, 88.2, 117.6, 147.0, and 176.4 psi) at a constant cross-flow of 30.4 cm/s. After adjusting the pressure, the membrane filtration unit was run for 1 h before taking samples for analysis.

After stabilizing the membrane (as described above) and prior to experiments with natural hormones, DI water (4 L) was introduced to the feed reservoir. The cross-flow and the permeate flux were adjusted to 30.4 cm/s and 15 μm/s (54 L m^{-2} h^{-1} or 32.4 gfd), respectively. Natural hormones were then spiked into the feed reservoir to make up a concentration of 100 ng/L. Feed and permeate samples (1 mL each) were taken for analysis at specified time intervals.

Mass Transfer Coefficient Measurement. The mass transfer coefficient, k_f, used in eq 9, was determined experimentally using the method described by Sutzkover et al. (*32*). Experiments were conducted at a cross-flow velocity of 30.4 cm/s (corresponding to a channel Reynolds number of 3650) by first measuring the pure water flux, then adding NaCl to the feed reservoir to make up a feed salt concentration of 0.1 M, and measuring the permeate flux and the permeate salt concentration. This procedure was carried out at two different applied pressures, 6 and 10 bar (88 and 147 psi), and was repeated for both the NF-270 and NF-90 membranes.

Knowing the permeate and feed salt concentrations (and thus, the corresponding osmotic pressures based on Van't Hoff equation, π_p and π_b, respectively), the applied pressure (ΔP), the pure water flux (J_w), and the permeate flux with the 0.1 M NaCl solution (J_{salt}) enables the evaluation of salt concentration at the membrane surface. This membrane surface concentration is used in the film model for concentration polarization to determine the mass transfer coefficient (*32*):

$$k_f = \frac{J_{salt}}{\ln\left[\frac{\Delta P}{\pi_b - \pi_p}\left(1 - \frac{J_{salt}}{J_w}\right)\right]} \qquad (12)$$

Results and Discussion

Estimation of NF Membrane Pore Size. Organic tracer real retention (R_r) was obtained from observed retention (R_o) after taking into account concentration polarization effects using eq 9 and the measured mass transfer coefficient, eq 12. Solute concentration polarization was quite severe at high permeate fluxes as indicated by the calculated ratio of solute membrane surface concentration to feed concentration; this ratio varied from 1.04 to 3.33 as the permeate flux increased from 12 to 45 μm/s. Real retentions of the organic tracers by the NF-90 and NF-270 membranes at different permeate fluxes (or transmembrane pressures) are summarized in Figure 3.

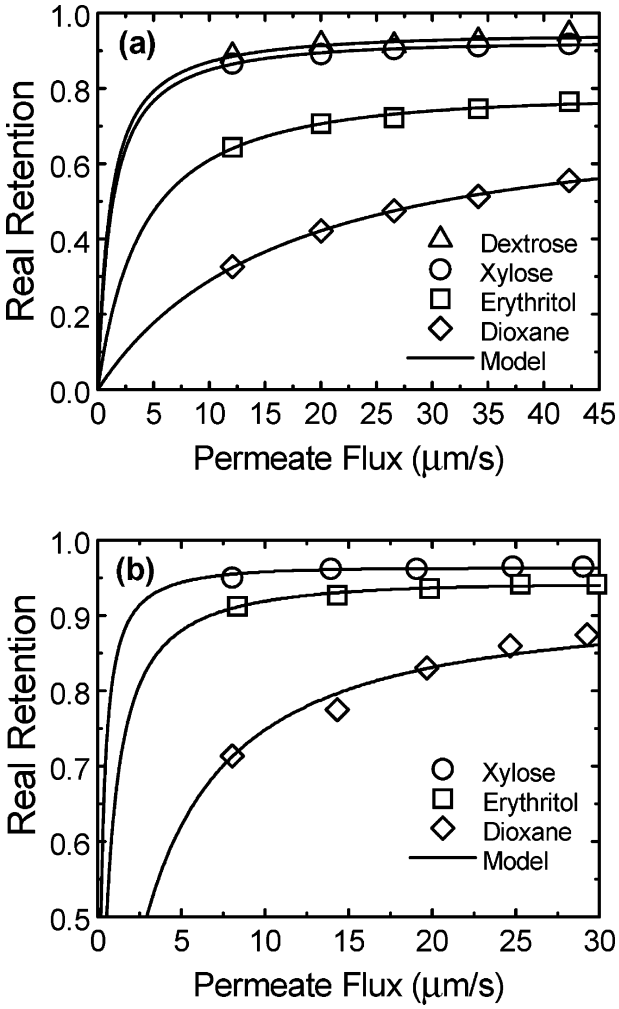

FIGURE 3. Real retention of the organic solute tracers as a function of permeate water flux for (a) NF-270 membrane and (b) NF-90 membrane. The symbols represent experimental data for the indicated organic solute tracers, while the solid lines represent the pore transport model predictions with the optimized parameters listed in Table 2. Feed solution contained 20 mg/L of organic tracer (as TOC) in deionized water. Other experimental conditions were as follows: cross-flow velocity = 30.4 cm/s, pH ≈ 6.0, and temperature = 20.0 °C. The permeate flux was varied by changing the applied pressure.

The obtained real retentions were used to estimate the NF membrane average pore size using the membrane pore transport model presented earlier. Since the model parameters ΦK_c and $Pe/\langle J_v \rangle$ ($= K_c L/\epsilon D_\infty K_d$ based on eq 5) are uniquely related to R_r, these parameters were determined by fitting the retention data to the model (eq 8) using an optimization procedure (Solver, Microsoft Excel). The parameters ΦK_c and $Pe/\langle J_v \rangle$ are a function of solely the variable λ (ratio of solute radius to membrane pore radius, r_s/r_p) and thus were used to obtain λ for each solute and membrane. With the determined value of λ and the given solute radius r_s, the membrane average pore radius was calculated for each organic tracer solute retention data as shown in Table 2.

The obtained pore radii are consistent for the different organic tracers. Based on these results, it is concluded that the NF-270 membrane has an average pore radius of 0.42 nm whereas the NF-90 has a pore radius of 0.34 nm. The results suggest that the NF-270 is "looser" than the NF-90, which is also reflected by its much lower NaCl retention.

TABLE 2. Nanofiltration Estimated Pore Radii Obtained from Organic Tracer Experiments

compound	r_s (nm)	$\lambda = r_s/r_p$	pore radius, r_p (nm)
	NF-90 Membrane		
xylose	0.290	0.826	0.35
erythitol	0.263	0.784	0.34
dioxane	0.234	0.689	0.34
average			0.34
	NF-270 Membrane		
dextrose	0.324	0.787	0.41
xylose	0.290	0.752	0.39
erythitol	0.263	0.600	0.44
dioxane	0.234	0.522	0.45
average			0.42

TABLE 3. Physicochemical Properties of Natural Hormones

hormone	MW (g/mol)	log K_{ow}[a]	solubility (mg/L)[b]	pK_a[c]
estradiol	272.4	4.01	13	10.4
estrone	270.4	4.54	13	10.4
testosterone	288.4	3.84	18−25[d]	
progesterone	314.5	4.63	na[e]	

[a] Estimated using HyperChem chemical molecular modeling package (Hypercube, Inc, Gainesville, FL). [b] Ref *53*. [c] Estimated from Hammet and Taft equations (*54*). [d] Ref *55*. [e] na, not available.

Previous experimental data estimating average pore radii for various NF membranes yielded comparable results (*33*−*36*).

Hormone Physicochemical Properties. Several physicochemical properties of the natural hormones are summarized in Table 3. Two of the hormones, estradiol and estrone, have phenolic groups with a pK_a value of 10.4, while the other two hormones, testosterone and progesterone, have no dissociable functional groups.

The interactions of a steroid hormone with chemical functional groups, such as those of membrane polymers, can be nonspecific (e.g., hydrophobic type) or specific (e.g., hydrogen bonding) (*37*). The former usually follows the polarity rule, whereby increasing the number of polar substituents decreases the binding potential. The latter depends on the type of the hormone functional groups and the spatial arrangement of these groups. Both of these interactions are very important in the biological action of steroid hormones (*37*).

All natural steroid hormones used in this study have moderately high octanol−water partitioning coefficient (log K_{ow}) and low water solubility (Table 3). The log K_{ow} values indicate that the hormones would readily adsorb to hydrophobic materials. However, a recent study showed that adsorption of hormones to natural organic matter (NOM) is not predominantly governed by hydrophobic interactions but rather closely related to hydrogen bonding (*38*). This is consistent with the fact that the steroid hormone progesterone binds to its receptor via hydrogen bonding (*39*). Several studies also indicated the possibility of hydrogen bonding between nonionic solutes and polyamide nanofiltration membranes (*19*, *40*).

Nanofiltration of Natural Hormones. Retention of organics by NF membranes can be attributed to a number of mechanisms, the most common of which are steric interaction (or size exclusion), charge exclusion (repulsion), and adsorption to the membrane surface. The natural hormones investigated in this study are undissociated at the pH of the experiments (pH 6), and only polar moieties contribute to the charge distribution within the molecule. Under these conditions, ionic (charge) interactions between the hormones and the membranes are absent, and steric exclusion and adsorptive effects are expected to dominate.

Figures 4−7 present the concentration of estradiol, estrone, testosterone, and progesterone in the permeate and feed as a function of time following filtration by the NF-270 and NF-90 membranes. Because natural hormones can adsorb (or partition) to the membrane polymer to some extent (*20*, *41*), it is not surprising to observe the continual decrease in feed concentration over a relatively long period of time. The feed concentration then stabilizes as the adsorption of hormones to the membrane reaches equilibrium. This phenomenon is consistently observed for all natural hormones with both the NF-270 and NF-90 membranes.

Adsorption (or partitioning) of natural hormones to the membrane is likely driven by hydrophobic or hydrogen bonding, but the exact nature of the interactions involved is not fully understood. Water flux through nanofiltration membranes, which are slightly "looser" than reverse osmosis membranes, depends not only on the membrane pore size but also on the water ability to form hydrogen bonding with the hydrophilic groups of the membrane polymer (*42*, *43*). Specific adsorption can result in permeate water flux decline if organics have higher proton donor capacity than water and, thus, can displace water from the hydrophilic sites of the membrane (*40*). However, flux decline was not observed in our experiments, which may be attributed to the very low concentration of the natural hormones used (100 ng/L).

The molecular weights of the natural hormones range from 270 to 315 g/mol (Table 3), which translates to an approximate Stokes radius of 0.5 nm (radius of equivalent sphere) using the Wilke and Chang and the Stokes−Einstein equations (*44*). This is larger than the average pore radius of the NF-270 and NF-90 membranes. Thus, one would expect the retention of the hormones to be nearly complete. When converting the feed and permeate concentration relationship (Figures 4−7) into observed retention (Figure 8), it appears that retention of the natural hormones is initially high, almost 100%. However, as pointed out earlier, this initially high retention is attributed to adsorption of natural hormones to the membrane polymer. The retention decreases continuously as hormone adsorption onto the polymeric membranes progresses and eventually stabilizes when equilibrium is achieved.

The permeate concentration of natural hormones (Figures 4−7) follows a characteristic breakthrough curve as often observed in an activated carbon packed-column adsorption. However, the breakthrough concentrations are small—ranging from less than 1 ng/L for progesterone to less than 10 ng/L for estradiol—indicating that size exclusion is still a significant retention mechanism when adsorption has reached equilibrium. Another notable observation is that there is no significant difference in the retention of hormones by the NF-270 and NF-90 membranes despite the obvious difference in their estimated pore size. This observation supports our hypothesis that there is an additional transport mechanism of natural steroid hormones, namely, partitioning and subsequent diffusion across the membrane as we discuss in detail later in this paper. Diffusion following partitioning of hormones to the membrane can result in lower retention as compared to inert organic solutes, which do not adsorb to the membrane. This hypothesis is examined by constructing a theoretical retention curve for inert organic solutes as described below.

Modeling Organic Tracer and Hormone Retention. If the solute−membrane interaction is purely steric, the observed retention, for a given membrane pore size and solute radius, can be modeled at any given pressure (or permeate flux) using the pore transport model presented earlier. On the basis of the average membrane pore radii in Table 2, the

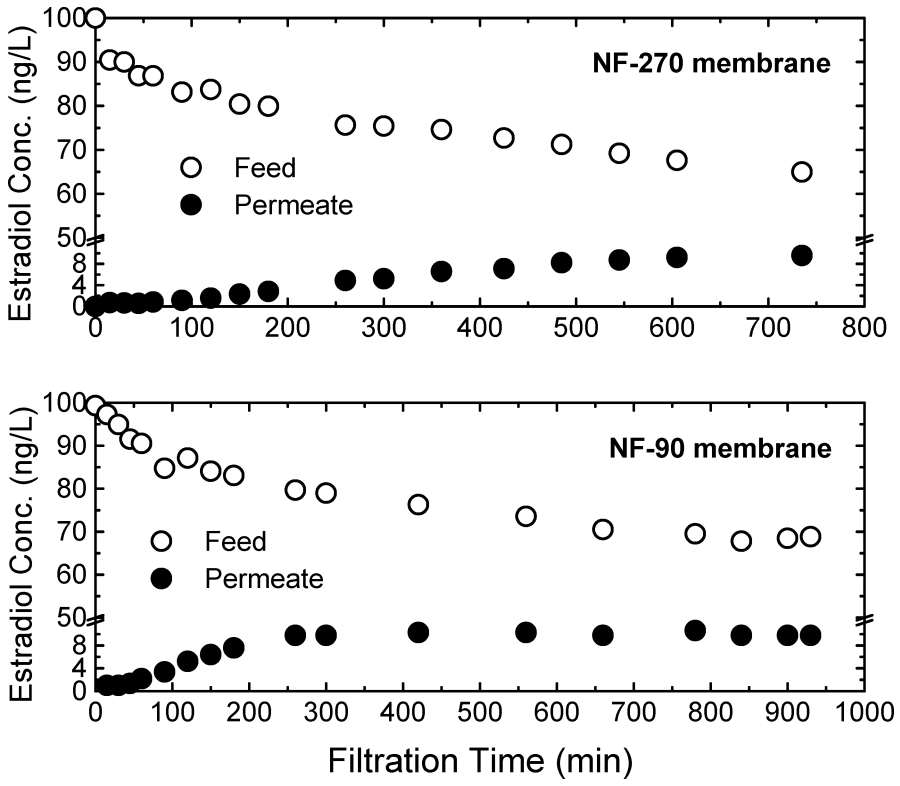

FIGURE 4. Permeate and feed concentrations of estradiol as a function of filtration time for the NF-270 membrane (top) and NF-90 membrane (bottom). The feed solution contained 100 ng/L estradiol in deionized water. Other experimental conditions were as follows: cross-flow velocity = 30.4 cm/s, permeate flux = 15 μm/s, pH $\approx$ 6.0, and temperature = 20.0 °C. During the nanofiltration run, the permeate and retentate were recirculated back to the feed reservoir.

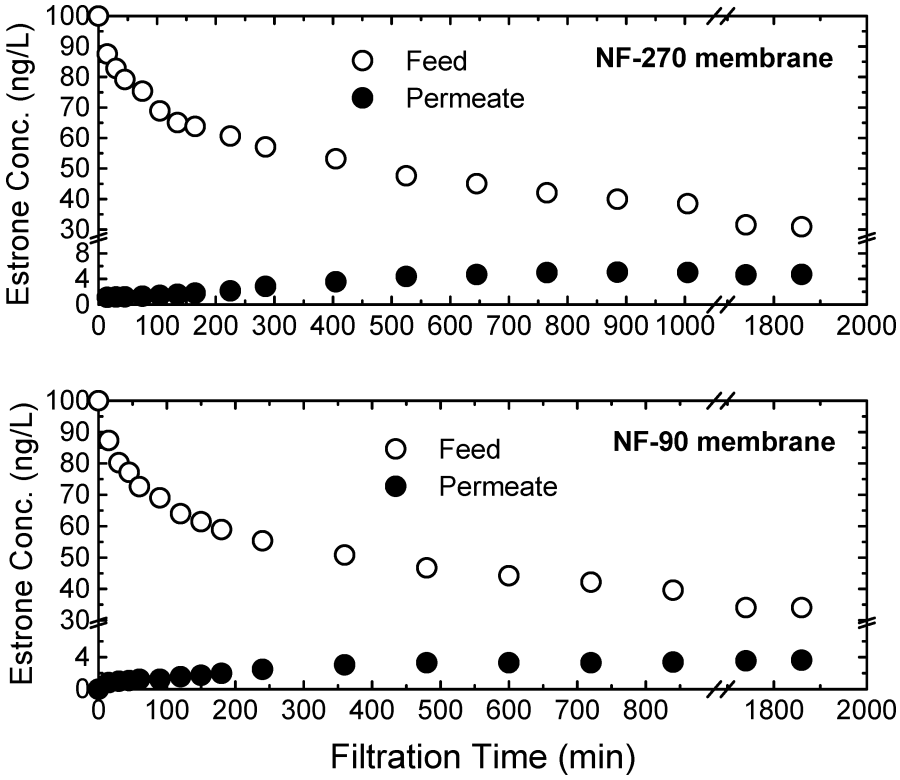

FIGURE 5. Permeate and feed concentrations of estrone as a function of filtration time for the NF-270 membrane (top) and NF-90 membrane (bottom). The feed solution contained 100 ng/L estrone in deionized water. Other experimental conditions were the following: cross-flow velocity = 30.4 cm/s, permeate flux = 15 μm/s, pH $\approx$ 6.0, and temperature = 20.0 °C. During the nanofiltration run, the permeate and retentate were recirculated back to the feed reservoir.

predicted observed retention of inert organic solutes by the NF-270 and the NF-90 membranes as a function of molecular weight, under conditions similar to those used for the natural hormone filtration experiments, is shown in Figure 9. The

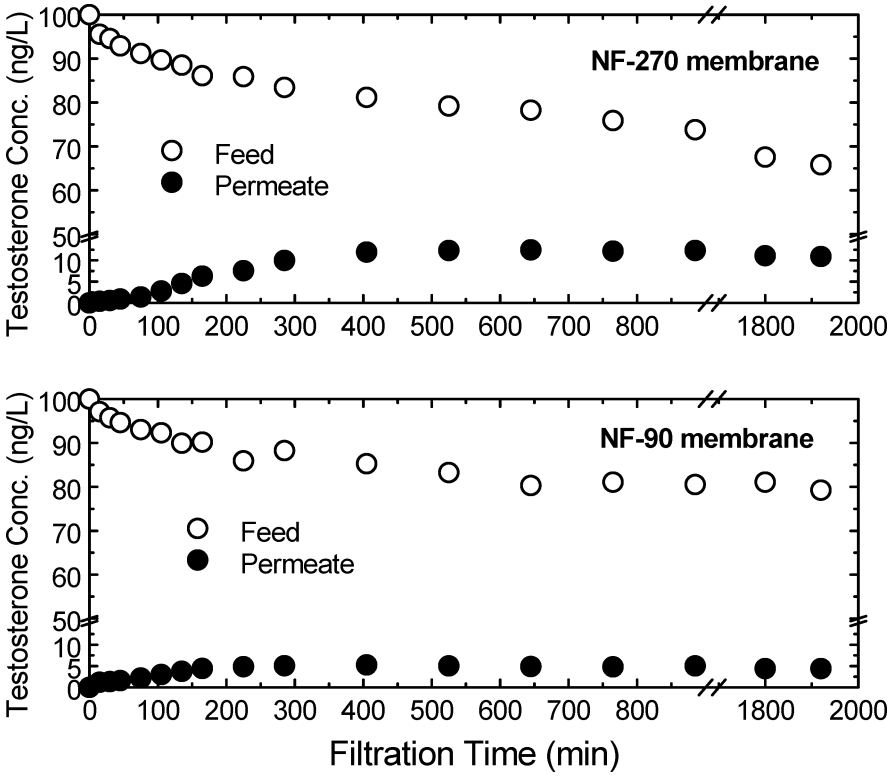

FIGURE 6. Permeate and feed concentrations of testosterone as a function of filtration time for the NF-270 membrane (top) and NF-90 membrane (bottom). The feed solution contained 100 ng/L testosterone in deionized water. Other experimental conditions were the following: cross-flow velocity = 30.4 cm/s, permeate flux = 15 μm/s, pH $\approx$ 6.0, and temperature = 20.0 °C. During the nanofiltration run, the permeate and retentate were recirculated back to the feed reservoir.

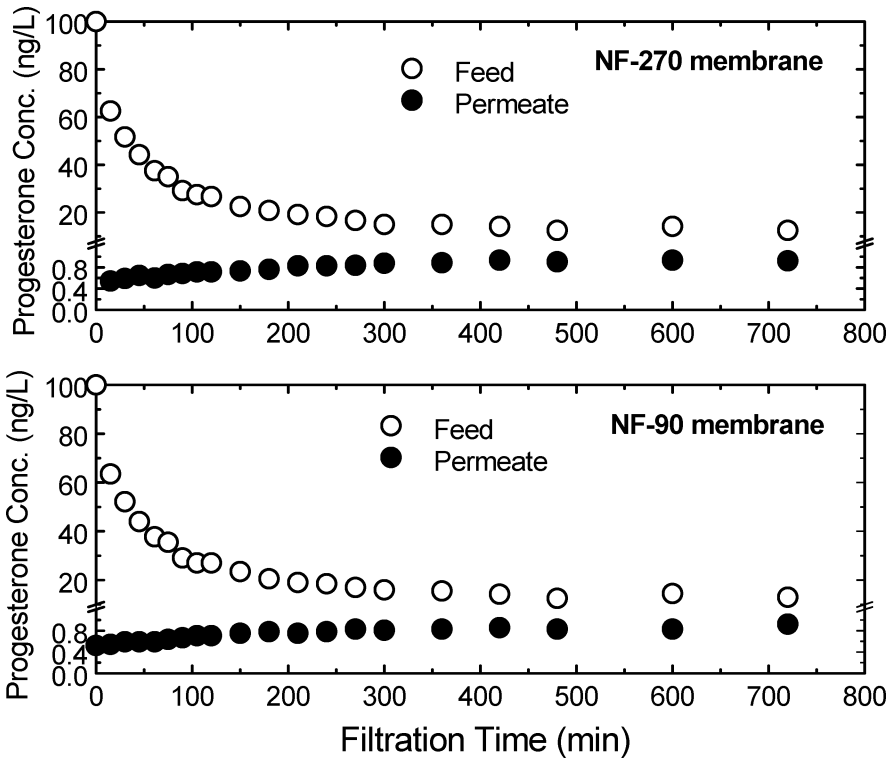

FIGURE 7. Permeate and feed concentrations of progesterone as a function of filtration time for the NF-270 membrane (top) and NF-90 membrane (bottom). The feed solution contained 100 ng/L progesterone in deionized water. Other experimental conditions were the following: cross-flow velocity = 30.4 cm/s, permeate flux = 15 μm/s, pH $\approx$ 6.0, and temperature = 20.0 °C. During the nanofiltration run, the permeate and retentate were recirculated back to the feed reservoir.

experimentally determined observed retentions of the four natural steroid hormones (taken at the end of the experiment when retention has been stabilized) are also included in this figure (symbols).

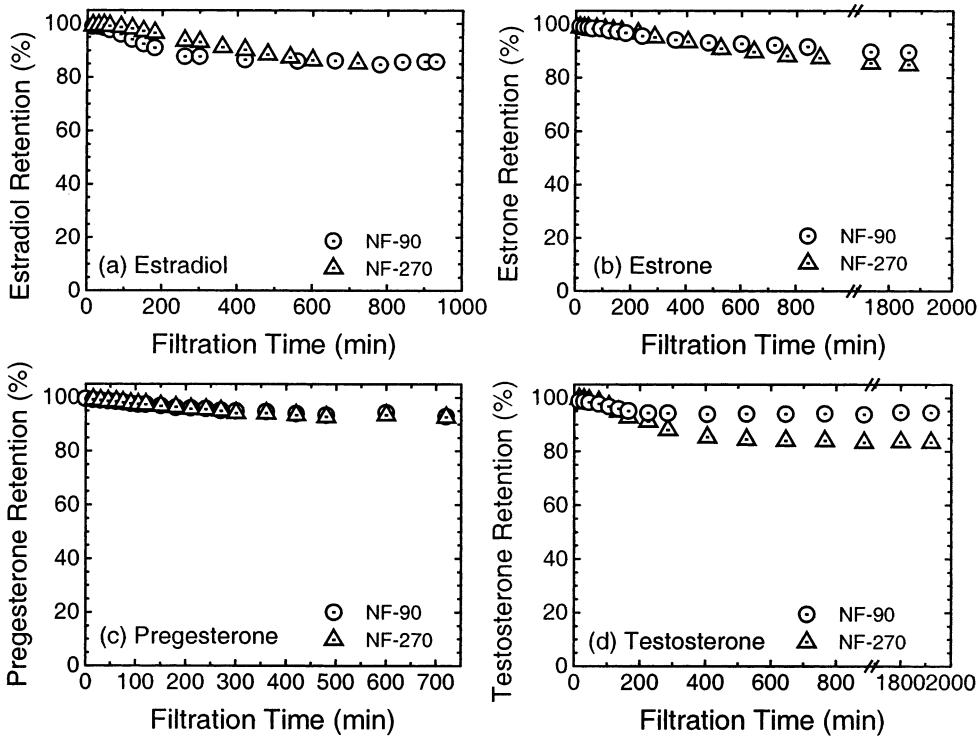

FIGURE 8. Percent retention of (a) estradiol, (b) estrone, (c) progesterone, and (d) testosterone by NF-270 and NF-90 as a function of time. The feed solution contained 100 ng/L of the corresponding hormone in deionized water. Other experimental conditions were the following: cross-flow velocity = 30.4 cm/s, permeate flux = 15 μm/s, pH $\approx$ 6.0, and temperature = 20.0 °C. During the nanofiltration run, the permeate and retentate were recirculated back to the feed reservoir.

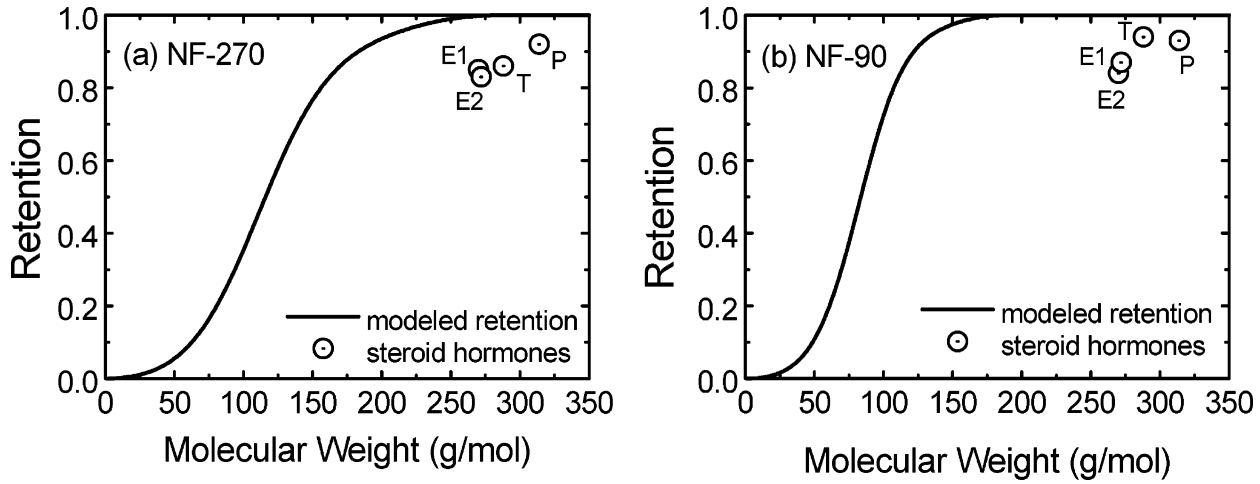

FIGURE 9. Model predictions (solid line) for observed retention of nonadsorptive inert organics as a function of solute molecular weight based on the pore transport model for (a) NF-270 membrane and (b) NF-90 membrane. Also included are the measured observed retentions of the four hormones (opens symbols): E1, estrone; E2, estradiol; T, testosterone; and P, progesterone. The observed retention of the steroid hormones was taken at the end of the adsorption stage (after 12 h). The relevant organic tracer parameters in Table 2 were used in the model calculations. Other parameters used in modeling were as follows: cross-flow velocity = 30.4 cm/s, permeate flux = 15 μm/s, and temperature = 20.0 °C.

While the model can predict the retention of inert organics (as shown earlier for our organic tracers), it overestimates the retention of natural hormones. It is postulated that this phenomenon is attributed to diffusive transport of natural hormones through the membrane polymer matrix. Natural hormones can dissolve or partition into the membrane active (skin) layer, then diffuse through the polymer via a sequence of "make-and-break" bonding with the membrane functional groups, and finally desorb at the permeate side (*45*). This mechanism, among others, is discussed below.

Hormone Retention Mechanisms. Hormone adsorption to the membrane is the predominant removal mechanism at the initial stage of filtration. For our experiments, this initial time corresponds to a cumulative permeate water flux of approximately 360 to 720 L/unit of membrane area. At the later stage, retention of natural hormones is lower than expected based purely on a steric or size exclusion mechanism.

Although size exclusion is the major separation mechanism at the later stages of filtration, we propose that partitioning and subsequent diffusion through the membrane polymer matrix results in a somewhat lower retention. In this process, the adsorption of natural hormones onto the membrane skin layer should be fast and, thus, not a rate-limiting step. Rather, the rate of steroid hormone transport across the membrane is governed by the diffusion through

the skin (active) layer of the thin-film composite NF membranes. A recent study suggests that the polyamide skin layer of the NF-270 is very thin, in the range of 15−40 nm, as compared to 200−300 nm for most RO membranes (*29*, *46*). Thus, although diffusive transport of steroid hormones through the membrane polymeric matrix is slow, a small but clear deviation of retention from the theoretical retention curve based on size exclusion is observed (Figure 9). Furthermore, the similar retention of natural hormones by the "tight" NF-90 and the "loose" NF-270 membranes can be explained if they have comparable active layer thicknesses.

A number of studies addressed the diffusion of hormones in both polymeric and biological membranes (*47*−*51*), mostly for drug delivery purposes. These studies can shed light on the retention mechanisms of the four hormones by the commercial NF membranes. The active skin layer of the NF-270 and NF-90 membranes is made of aromatic polyamide (*29*). Water is sparsely soluble in the polymer, and the diffusion process of natural hormones in the membrane takes place in a polymeric matrix saturated with small amounts of water. Although convective flow has only a small contribution to the transport of natural hormones across the membrane, the presence of water is thought to play an important role in facilitating the diffusion process. Diffusion of hormones in the dense polymeric phase is accomplished by a series of successive jumps from one equilibrium position to another, which usually involve the formation and breakage of secondary bonds (*52*). Such make-and-break action can be the result of switching between two bonding sites or between a hydrophobic bond to a substrate and a hydrogen bond to water (*37*, *47*). Both hydrophobic and hydrogen bonds have activation energies in the range of approximately 15 kJ/mol. In comparison, at room temperature the molecule kinetic (thermal) energy amounts to 2.5 kJ/mol, which means that such individual bonds can make-and-break quite readily (*37*). Several studies have demonstrated that such a process is temperature sensitive and that permeation of hormones through various membranes depends strongly on temperature in the tested range of 10−50 °C (*47*−*49*).

Acknowledgments

The authors acknowledge the support of the US National Science Foundation (Grant BES 0114527), and the University of Wollongong and the Australian Institute of Nuclear Science and Engineering for a doctoral scholarship to L.D. Nghiem.

Literature Cited

(1) Johnson, A. C.; Sumpter, J. P. *Environ. Sci. Technol.* **2001**, *35*, 4697−4703.
(2) Kolpin, D. W.; Furlong, E. T.; Meyer, M. T.; Thurman, E. M.; Zaugg, S. D.; Barber, L. B.; Buxton, H. T. *Environ. Sci. Technol.* **2002**, *36*, 1202−1221.
(3) Shen, J. H.; Gutendorf, B.; Vahl, H. H.; Shen, L.; Westendorf, J. *Toxicology* **2001**, *166*, 71−78.
(4) Tabata, A.; Kashiwada, S.; Ohnishi, Y.; Ishikawa, H.; Miyamoto, N.; Itoh, M.; Magara, Y. *J. Water Sci. Technol.* **2001**, *43*, 109−116.
(5) Ternes, T. A. *Trends Anal. Chem.* **2001**, *20*, 419−434.
(6) Purdom, C. E.; Hardiman, P. A.; Bye, V. J.; Eno, N. C.; Tyler, C. R.; Sumpter, J. P. *J. Chem. Ecol.* **1994**, *8*, 275−285.
(7) Facemire, C. F.; Gross, T. S.; Guillette, L. T. *Environ. Health Perspect.* **1995**, *103*, 79−86.
(8) Carey, C.; Bryant, C. J. *Environ. Health Perspect.* **1995**, *103*, 13−18.
(9) Harries, J. E.; Sheahan, D. A.; Jobling, S.; Matthienssen, P.; Neall, P.; Sumpter, J. P.; Tylor, T.; Zaman, N. *J. Environ. Toxicol. Chem.* **1997**, *16*, 534−542.
(10) Ottinger, M. A.; Abdelnabi, M.; Quinn, M.; Golden, N.; Wu, J.; Thompson, N. *Neurotoxicol. Teratol.* **2002**, *24*, 17−28.
(11) Michael, J. *Occup. Med. Educ.* **2001**, *58*, 281−288.
(12) Solomon, G. M.; Schettler, T. *Can. Med. Assoc. J.* **2000**, *163*, 1471−1476.
(13) Hess, R. A.; Bunick, D.; Lee, K.-H.; Barh, J.; Taylor, J. A.; Korach, K. S.; Lubahn, D. B. *Lett. Nature* **1997**, *390*, 509−512.
(14) Higgins, J.; Warnken, J.; Sherman, P. P.; Teasdale, P. R. *Water Res.* **2002**, *36*, 5045−5056.
(15) Van der Bruggen, B.; Schaep, J.; Wilms, D.; Vandecasteele, C. *J. Membr. Sci.* **1999**, *156*, 29−41.
(16) Berg, P.; Hagmeyer, G.; Gimbel, R. *Desalination* **1997**, *113*, 205−208.
(17) Van der Bruggen, B.; Schaep, J.; Maes, W.; Wilms, D.; Vandecasteele, C. *Desalination* **1998**, *117*, 139−147.
(18) Kiso, Y.; Nishimura, Y.; Kitao, T.; Nishimura, K. *J. Membr. Sci.* **2000**, *171*, 229−237.
(19) Schäfer, A. I.; Nghiem, D. L.; Waite, T. D. *Environ. Sci. Technol.* **2003**, *37*, 182−188.
(20) Nghiem, D. L.; Schäfer, A. I. *Environ. Eng. Sci.* **2002**, *19*, 441−451.
(21) Kedem, O.; Katchalsky, A. *Biochim. Biophys. Acta* **1958**, *27*, 229−246.
(22) Deen, W. M. *AIChE J.* **1987**, *33*, 1409−1424.
(23) Kiso, Y.; Kon, T.; Kitao, T.; Nishimura, K. *J. Membr. Sci.* **2001**, *182*, 205−214.
(24) Kiso, Y.; Kitao, T.; Jinno, K.; Miyagi, M. *J. Membr. Sci.* **1992**, *74*, 95−103.
(25) Lightfood, E. N.; Bassingthwaighte, J. B.; Grabowski, E. F. *Ann. Biomed. Eng.* **1976**, *4*, 78−90.
(26) Zeman, L. J.; Zydney, A. L. *Microfiltration and Ultrafiltration: Principles and Applications*; Marcel Dekker: New York, 1996.
(27) Song, L.; Elimelech, M. *J. Chem. Soc., Faraday Trans.* **1995**, *91*, 3389−3398.
(28) Bungay, P. M.; Brenner, H. *Int. J. Multiphase Flow* **1973**, *1*, 25−56.
(29) Freger, V.; Gilron, J.; Belfer, S. *J. Membr. Sci.* **2002**, *209*, 283−292.
(30) John, J. Sigma Aldrich, Australia, 2002, personal communication.
(31) Kavalcik, L. Perkin-Elmer, USA, 2003, personal communication.
(32) Sutzkover, I.; Hasson, D.; Semiat, R. *Desalination* **2000**, *131*, 117−127.
(33) Seidel, A.; Waypa, J.; Elimelech, M. *Environ. Eng. Sci.* **2001**, *18*, 105−113.
(34) Vrijenhoek, E. M.; Waypa, J. J. *Desalination* **2000**, *130*, 265−277.
(35) Van der Bruggen, B.; Schaep, J.; Wilms, D.; Vandecasteele, C. *Sep. Sci. Technol.* **2000**, *35*, 169−182.
(36) Wang, X.-L.; Tsuru, T.; Nakao, S.-I.; Kimura, S. *J. Membr. Sci.* **1997**, *135*, 19−32.
(37) King, R. J. B.; Mainwaring, W. I. P. *Steroid-Cell Interactions*; Buetterworths: London, 1974.
(38) Yamamoto, H.; Liljestrand, H. M.; Shimizu, Y.; Morita, M. *J. Environ. Sci. Technol.* **2003**, *37*, 2646−2657.
(39) Le Questel, J.; Boquet, G.; Berthelot, M.; Laurence, C. *J. Phys. Chem.* **2000**, *104*, 11816−11823.
(40) Williams, M. E.; Hestekin, J. A.; Smothers, C. N.; Bhattacharyya, D. *Ind. Eng. Chem. Res.* **1999**, *38*, 3683−3695.
(41) Nghiem, L. D.; Schafer, A. I.; Waite, T. D. *Water Sci. Technol.* **2002**, *46*, 265−272.
(42) Scherer, J. R.; Bailey, G. F. *J. Membr. Sci.* **1983**, *13*, 43−52.
(43) Scherer, J. R.; Bailey, G. F. *J. Membr. Sci.* **1983**, *13*, 29−41.
(44) Geankoplis, C. J. *Transport Processes and Unit Operations*, 3rd ed.; Prentice-Hall: Englewood Cliffs, NJ, 1993.
(45) van den Berg, G. B.; Smolders, C. A. *J. Membr. Sci.* **1992**, *73*, 103−118.
(46) Freger, V. *Langmuir* **2003**, *19*, 4791−4797.
(47) Cohen, B. E. *J. Membr. Biol.* **1975**, *20*, 205−234.
(48) Arrowsmith, M.; Hadgraft, J.; Kellaway, I. W. *Int. J. Pharm.* **1983**, *14*, 191−208.
(49) Liu, J. C.; Sun, Y.; Tojo, K.; Chien, Y. W. *Int. J. Pharm.* **1985**, *25*, 265−274.
(50) Leong, K. W.; Langer, R. *Adv. Drug Delivery Rev.* **1987**, *1*, 199−233.
(51) Couarraze, G.; Leclerc, B.; Conrath, G.; Falson-Rieg, F.; Puisieux, F. *Int. J. Pharm.* **1989**, *56*, 197−206.
(52) Glasstone, S.; Laidler, K. J.; Eyring, H. *The Theory of Rate Processes*; McGrawHill Book Co: New York, 1941.
(53) Lai, K. M.; Johnson, K. L.; Scrimshaw, M. D.; Lester, J. N. *Environ. Sci. Technol.* **2000**, *34*, 3490−3494.
(54) Perrin, D. D. In *Physical Chemical Properties of Drugs*; Yalkowsky, S. H., Sinkula, A. A., Valvani, S. C., Eds.; Marcel Dekker: New York, 1980.
(55) Sugaya, Y.; Yoshiba, T.; Kajima, T.; Ishihama, Y. *Pharm. Soc. Jpn.* **2002**, *122*, 237−246.

Received for review August 31, 2003. Revised manuscript received November 10, 2003. Accepted January 9, 2004.

ES034952R